

# SMART PHASE-ONLY MICROMIRROR ARRAY FABRICATED BY STANDARD CMOS PROCESS

Adisorn Tuantranont, Victor M. Bright, Li-Anne Liew, Wenge Zhang, and Y.C. Lee

NSF Center for Advanced Manufacturing and Packaging  
of Microwave, Optical, and Digital Electronics (CAMPmode)

Dept. of Mechanical Engineering, University of Colorado, Boulder, CO, USA 80309-0427

Adisorn.Tuantranont@colorado.edu; Tel.(303)735-1763 (phone); (303)492-3498 (FAX)

## ABSTRACT

Smart, phase-only modulation micromirror arrays have been implemented through a commercial CMOS service. The novel, 2-dimensional array of deflectable micromirrors with integrated CMOS switching circuits and piezoresistive deflection sensors on flexures is presented in this paper. The individual mirror pixels are capable of modulating light in the visible to near-infrared spectrum by piston-like movement of a trampoline-type suspended micromirror driven by thermal multi-morph actuators. A flip chip bonding technology is used to integrate the micromirror array with a microlens array to increase the optical fill factor of the hybrid system. Finite element analysis is used to model electro-thermo-mechanical behavior of micromirror. The 2.5 mrad beam steering angle was successfully demonstrated.

## INTRODUCTION

The use of industrial CMOS technology enables the cointegration of mechanical microstructures with integrated circuits on the same chip. New generation of Micro-Electro-Mechanical Systems (MEMS), which is smarter and more concise is achieved by integration of digital or analog signal amplifying and processing IC circuits right next to the MEMS devices. Smart, phase-only micromirror array is a promising integrated microsystem that leads to many applications such as optical beam steering, optical data interconnect, real-time image recognition, optical interferometer, spectroscopy and aberration correction. Large deflection of micromirror is required to be able to modulate light in infrared wavelength. From many previous works on micromirrors, surface micromachining was used to fabricate parallel plate structure for electrostatic driven micromirrors [1]. Due to a narrow gap between the electrodes, the mirror's deflection achieved is in the range of submicrometer, which is not adequate to modulate light in longer wavelength than visible spectrum. Bulk micromachined micromirror is a promising technique to solve this limitation. In this paper, a novel phase-only

micromirror array including on-chip circuitry and mirror structure was fabricated through standard CMOS process using SCNA\_MEMS technology [2]. In addition to the long travel range, other advantages of CMOS micromirror include low cost, high yield, mass production, and easy integration of digital or analog electronics in a standard integrated circuit process. The finite element analysis and modeling of thermal multi-morph actuator are described in detail. The usefulness of device for optical beam steering applications is demonstrated.

## CMOS MICROMIRROR

The novel 2-dimensional array of deflectable micromirrors (Figure 1) is fabricated by the Orbit 2  $\mu\text{m}$  double polysilicon, double metal CMOS process, available through the MOS Implementation Service (MOSIS).

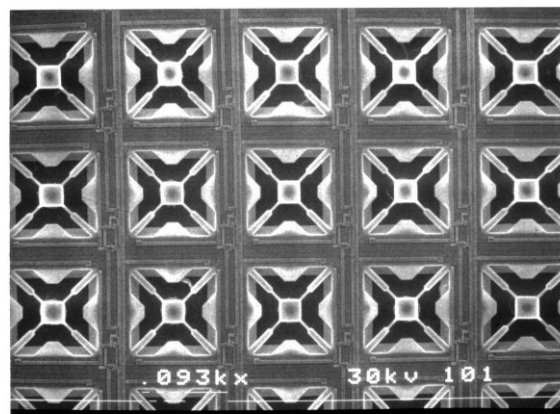


Figure 1. A portion of smart phase-only modulation micromirror array.

The micromirror is designed to modulate light in the visible to near-infrared wavelengths by piston-type movement of micromirror. The individual mirror pixel consists of a  $40\text{ }\mu\text{m} \times 40\text{ }\mu\text{m}$  trampoline-type micromirror plate suspended by thermal multi-morph flexures on each corner, as shown in Figure 2(a). The suspended micromirror plate composes of stacked aluminum commonly available in standard IC processes. The

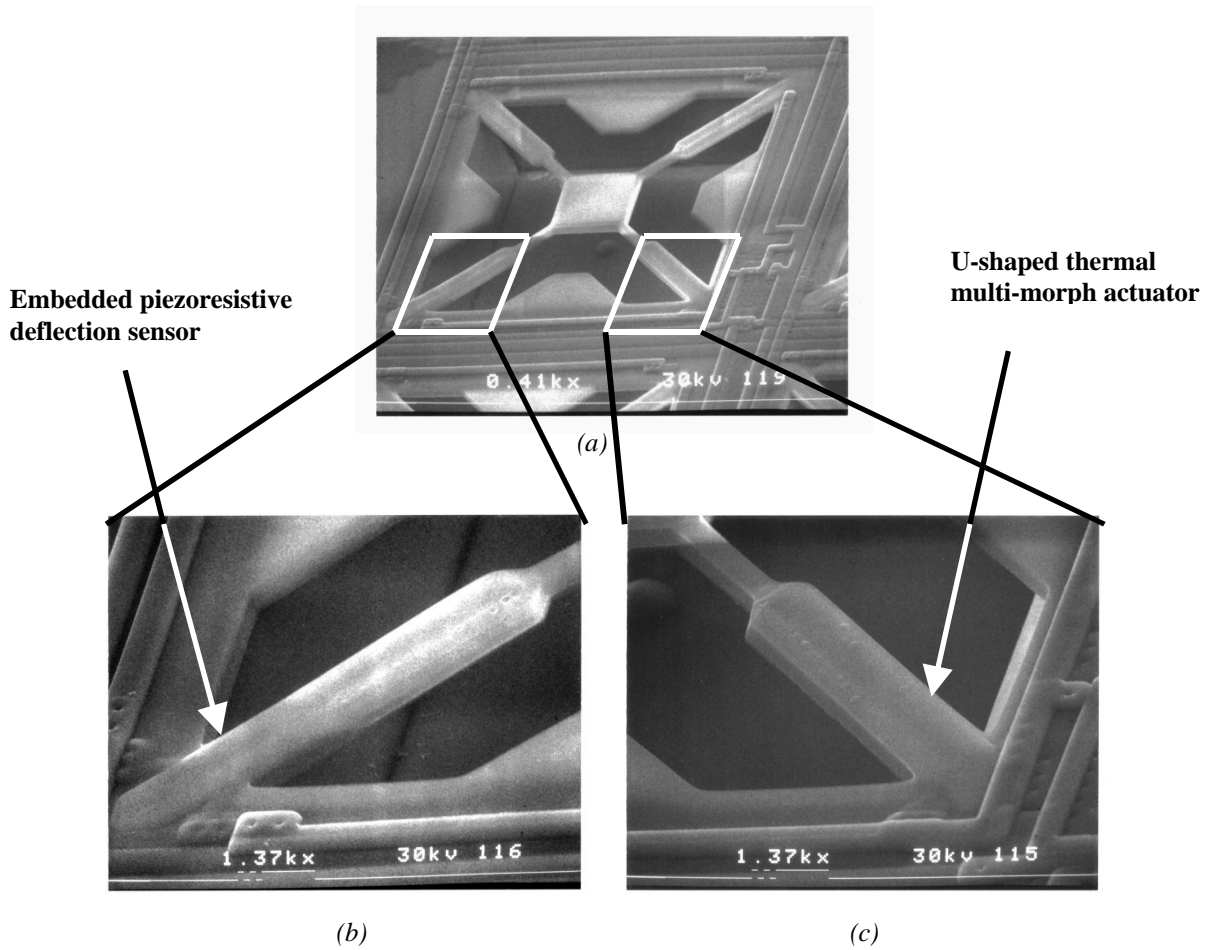


Figure 2. Scanning electron micrograph of a pixel of smart micromirror array (a), the piezoresistive deflection sensor embedded in the flexure (b), and a thermal multi-morph actuator in the flexure (c).

aluminum shows a high optical reflectivity ( $>90\%$ ) over operation wavelengths. The micromirror plate and multi-morph actuators are coupled with an oxide spring beam. The thermal multi-morph structures consist of polysilicon resistor wires and aluminum layers encapsulated in  $\text{SiO}_2$ , as shown in Figure 2(c). Due to the different coefficients of thermal expansion of multi-layer sandwich of different materials, the flexures curl when an ohmic heating from the input electrical power is applied [3], thus causing piston-type motion of the micromirror plate. The array is anisotropically etched in EDP solution to release the micromirror structure. A pit is formed under the suspended pixel structure, giving high degree of thermal isolation from the surrounding substrate. Piezoresistive deflection sensors, as shown in Figure 2(b), are integrated on flexures of each micromirror to provide feedback control of the position of each micromirror to improve device performance in real-time. Integrated CMOS switching circuit adjacent to each pixel, as shown in Figure 3, allows to address the pixel by 5 V data pulses and operate in digital mode.

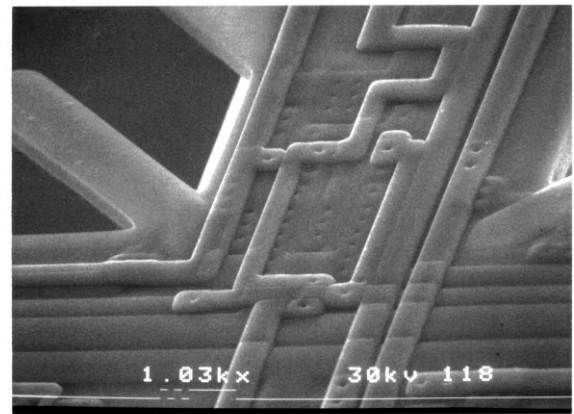


Figure 3. Integrated CMOS switching circuit adjacent to each pixel allowing digital mode operation.

The multi-morph beam is  $72\ \mu\text{m}$  long and  $14\ \mu\text{m}$  wide with  $2.8\ \mu\text{m}$  wide polysilicon heater wire running between aluminum layer and oxide layer to generate heat. The ends of multi-morph actuator beams are

coupled to the micromirror plate with the oxide beams (21  $\mu\text{m}$  long and 7  $\mu\text{m}$  wide). After the anisotropic silicon etch has undercut and released the cantilever beams, the beams curled up out of the substrate plane due to internal stresses in their thin structural layers. The micromirror plate is thus elevated above the substrate plane.

## DESIGN ANALYSIS

A simulation of the micromirror was conducted with a commercially available finite element analysis tool. The model consists of stacked layers of solid elements with thickness that corresponds to the actual structural layers fabricated. The analysis consists of an electro-thermal analysis to obtain the temperature distribution resulting from an input power. This is then coupled to a mechanical analysis in which the temperature distribution is used to determine deflections resulting from thermal expansion mismatch in a multi-morph structure.

### Electro-Thermal Analysis

An input voltage was applied to the polysilicon heating resistors of micromirror model, which correspond to the two thermal actuators. The other two of the four flexures contain piezoresistors for measuring mirror deflection. Heat transfer paths considered were the thermal conduction to the substrate and to the surrounding air. Both the air and substrate were assumed to remain at room temperature. Radiation was not considered because it has a negligible effect [4]. Only the steady state condition was considered in the analysis, corresponding to a static deflection of micromirror. The finite element simulation showing the temperature distribution is shown in Figure 4.

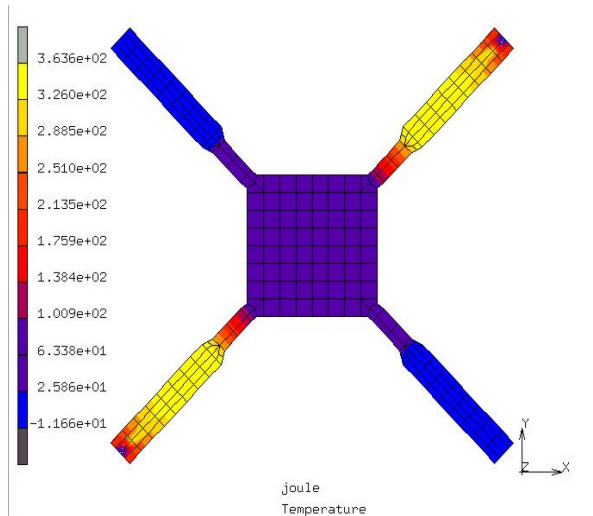


Figure 4. The electro-thermal finite element analysis showing the thermal distribution in the two actuator beams.

### Thermal-Mechanical Analysis

The temperature distribution resulting from the electro-thermal analysis was used as an input condition for the thermal-mechanical analysis. Figure 5 shows the finite element structural model of the micromirror when it is deflecting. Boundary condition is used to fix the location of the beam's base.

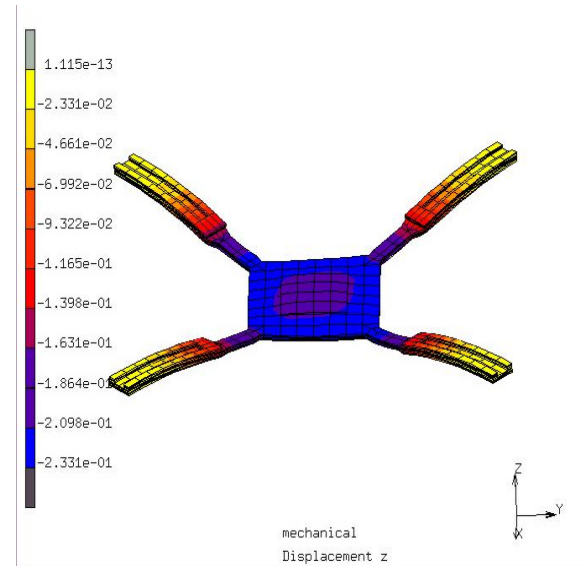


Figure 5. The finite element analysis of mirror deflection.

A comparison of measured results of micromirror's deflection with finite element analysis is shown in Figure 6.

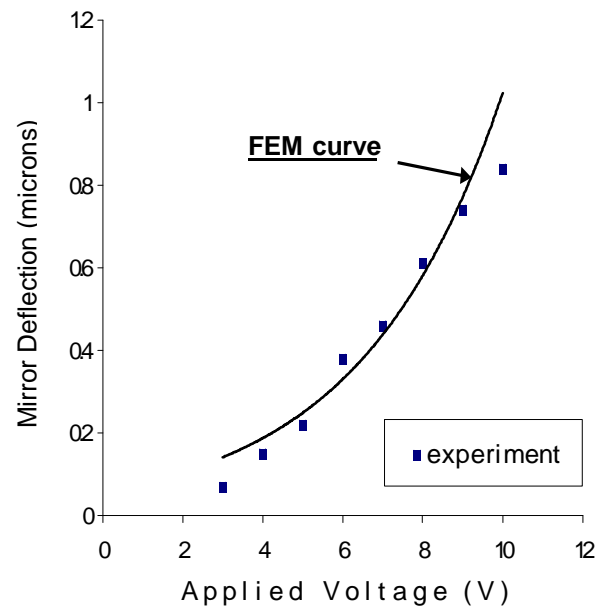


Figure 6. Mirror deflection versus applied voltage.

# MICROMIRROR CHARACTERIZATION

## Static Characterization

### Micromirror Deflection

Measurements were taken to determine the maximum possible deflection of the micromirror, and the deflection of micromirror versus applied power. Deflection of micromirror was measured over a range of input power by white light interferometer microscope. Measurements were taken on the center of micromirror. Figure 7 shows the experimentally determined mirror deflection versus applied power. The mirror deflection depends linearly on the drive power with maximum power of 150 mW per pixel at 2  $\mu\text{m}$  deflection.

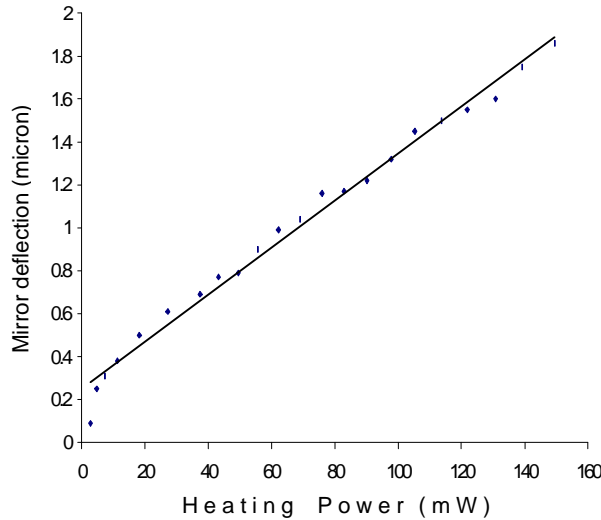


Figure 7. Micromirror deflection versus heating power.

### Piezoresistive detection

Deflection of the micromirror is detected with two piezoresistors embedded in the opposing beams. The position of the piezoresistors is at the clamped edges of the beams, where the mechanical stress is highest. The measured change of resistivity in a piezoresistor related to the mirror deflection as a linear relation is shown in Figure 8. Through Figure 8 a known relationship may be established to provide the feedback signal for real-time control of micromirror.

## Dynamic Characterization

Dynamic measurements were taken to determine the maximum operating frequency of the micromirror. Laser interferometer, shown in Figure 9, was setup and used to determine the time required to heat and cool the multi-morph beams. The micromirror was driven by a 4 Hz, 5 volt peak input signal. Figure 10 shows the

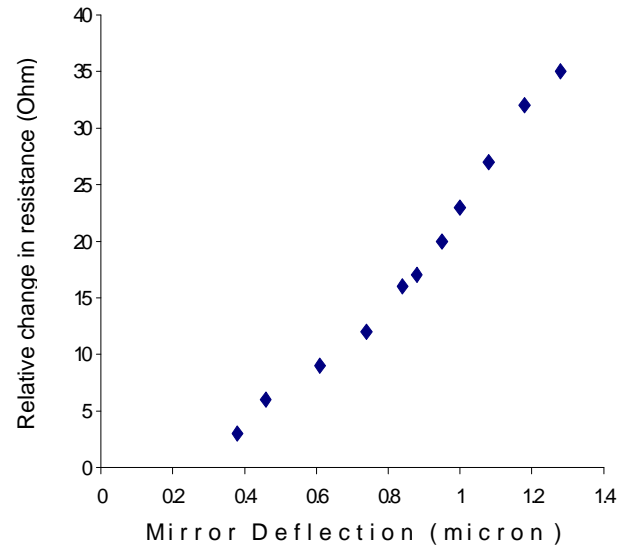


Figure 8. Mirror deflection versus relative change in resistivity of a piezoresistor.

driving input signal and output signal from photodetector. The upper trace indicates the square wave input and the lower trace indicates the interference fringe movement. The onset of heating or cooling of the beam occurs immediately after applied voltage changes. After the multi-morph beam reaches a steady state temperature, the micromirror stops moving and interference pattern stops changing. The heat and cool times for the multi-morph beam are 3 ms, but the encountered force of the oxide beam spring during micromirror actuation results in an increase of heating time to 7 ms. The maximum operating frequency of 100 Hz is achieved. Below this frequency, the multi-morph will completely heat and cool following the drive signal. Above this maximum frequency, multi-morph beam will not have adequate time to heat and cool and so will not completely deflect in either direction.

## MICROMIRROR/MICROLENS INTEGRATION

Using the refractive lenslet array to focus the incident light beam onto only the reflective surface of the mirror is the way to greatly improve the effective fill factor with corresponding decrease in static background interference effect. The micromirror in this experiment was designed specifically for use with an available commercial refractive lenslet array from Nippon Sheet Glass Company. Two-dimensional Planar Micro Lens (PML) is integrated directly on top of the micromirror array. Each lens has a circular shape 0.25 mm in diameter. The 250  $\mu\text{m}$  center-to-center spacing of the lens array matches with the center-to-center spacing of the micromirror array. The back focal length of the microlens is 0.56 mm. This lenslet array can provide

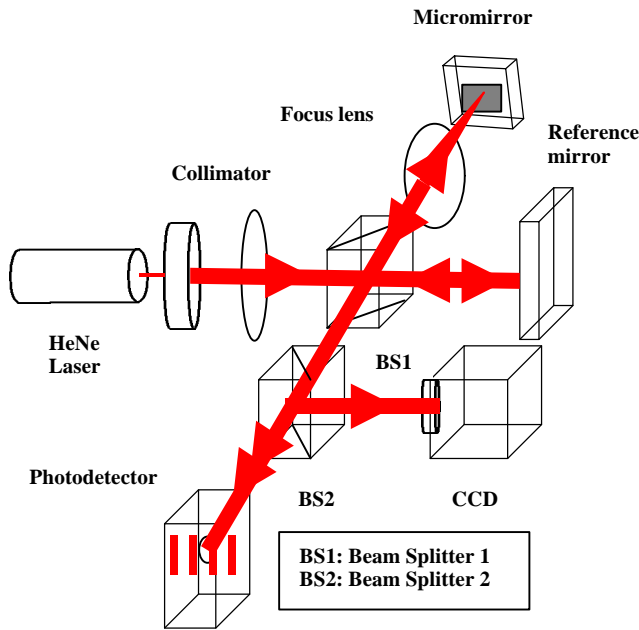


Figure 9. Laser interferometer experimental setup for frequency measurement.

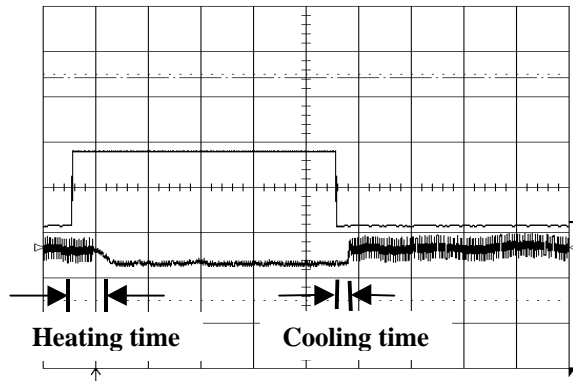


Figure 10. Experimental result showing input square wave and output interferometer data.

approximately 90 percent light transmission at visible wavelengths.

Hybrid flip chip assembly is applied to integrate the lenslet array on top of the micromirror array. Two glass spacers of 1.925 mm thickness and 1 mm x 14 mm were attached to the 16.5 mm x 14 mm quartz window with 20  $\mu$ m thick UV curable epoxy. The lenslet array was flipped and attached to the quartz window by UV curable epoxy. The quartz window with lenslet array was flip chip attached to the micromirror package and pre-cured under UV light. The alignment was then adjusted manually in the X and Y position. Afterward, the lenslet array integrated micromirror was investigated under interferometric microscope. Fringe patterns observed by the interferometric microscope were used to correct possible tilt alignment of the lenslet array. The focal point of lenslet was aligned on

the center of the micromirror, afterward the epoxy was cured firmly. From observation, the gap between the microlens and micromirror was controlled by the spacers accurately and equals to the focal length of the microlens. Figure 11 shows the close-up of the flip-chip integrated lenslet array on top of the micromirror array. The final device was packaged in a 40 pin dual-in-line (DIP) package as shown in Figure 12.

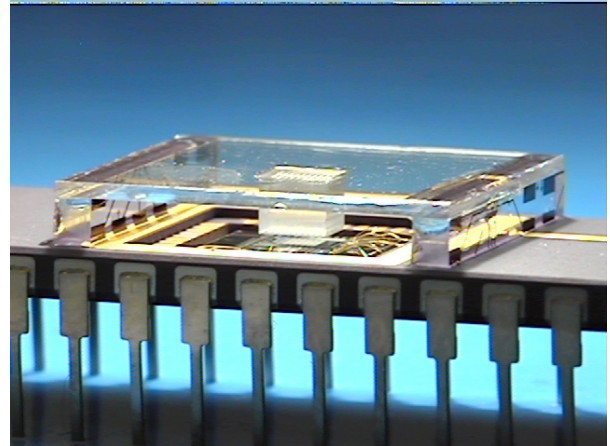


Figure 11. The lenslet array flip chip integrated on top of the micromirror array using glass spacers for gap control.



Figure 12. The final device packaged in a 40 pin DIP package.

## PHASED ARRAY BEAM STEERING

The optical experimental setup shown in Figure 13 was used to measure the far-field diffraction pattern of tested lenslet integrated micromirror for beam steering or aberration correction. The collimated HeNe laser was used as a signal light source. The beam is folded by mirror  $M_1$  into the optical characterization branch. The beam enters a beam splitter (BS1) and is redirected toward the lenslet integrated micromirror by passing through a pair of lenses  $L_1$  and  $L_s$  between BS1 and the lenslet integrated micromirror. An iris is located in front



of BS1 a focal length away from lens  $L_1$  to control beam diameter. The light from the lenslet integrated micromirror is reflected back through the afocal telescope ( $L_1$  and  $L_8$ ), BS1 and translating lenses  $L_{t1}$  and  $L_{t2}$ . The beam enters a Fourier transforming lens  $L_F$  and generates the far-field diffraction (point spread function, PSF) on a 256 x 256 pixel CCD camera. Focal lengths of lenses and specification of optical component locations in the experimental setup are listed in [1].

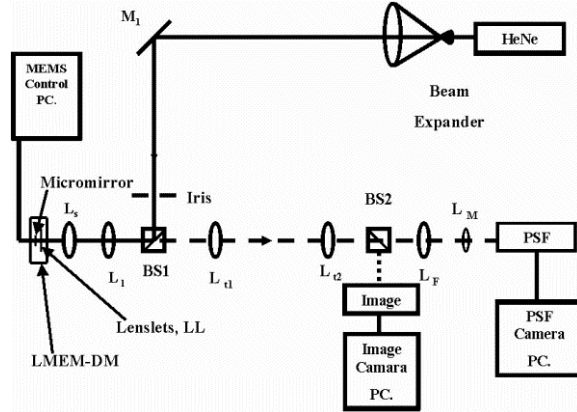


Figure 13. The optical experimental setup used to measure the far-field diffraction pattern.

In one dimension an optical phased array of  $n$  elements, with uniform phase shift spacing (between elements) from 0 to  $2\pi$  radians, steers a beam to an angle  $q_s = l/nL$ , where  $L$  is the spacing of the elements (in this case the lenslet dimension), and  $l$  is the operating wavelength. Beam steering of 2.5 mrad from boresight (Figure 14 and Figure 15) is implemented by a stepped linear ramp pattern across the columns of the micromirror. Steering angle measurements show excellent agreement (within 1% error) with one-dimensional beam steering theory.

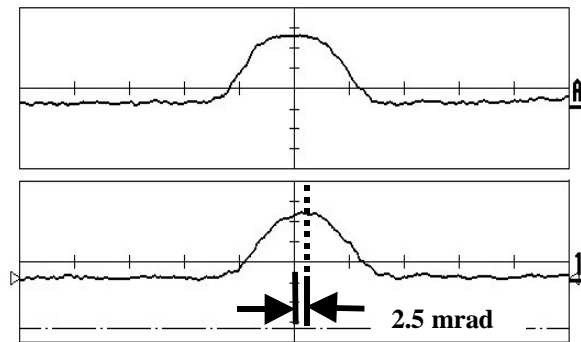


Figure 14. The beam profiles of unsteered (trace A) and steered beam (trace I).

## CONCLUSION

The phase-only micromirror array has been successfully fabricated by standard CMOS process. The micromirror is actuated by thermal multi-morph actuators and

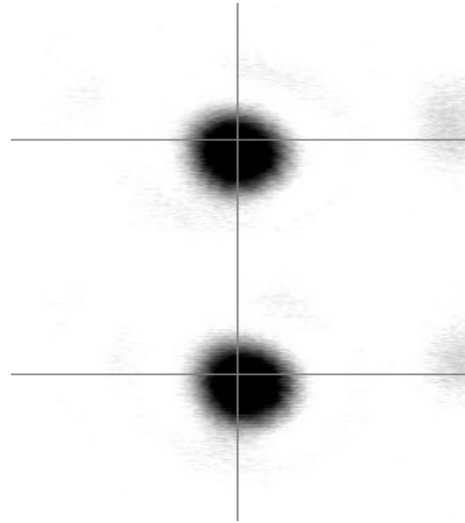


Figure 15. Central maximum beam steering for a 16 element micromirror array.

deflection is detected by piezoresistors. The CMOS switching circuit is integrated adjacent to the individual pixel to operate in digital mode. Lenslet array is flip chip integrated on top of the micromirror to increase the optical fill factor of the system. The hybrid mirror/lenslet array can modulate the light in visible to near infrared wavelengths. The device is used to demonstrate optical beam steering ability up to 2.5 mrad.

## ACKNOWLEDGEMENTS

This work was sponsored by the Air Force Office of Scientific Research (AFOSR), Grant # F49620-98-1-0291. Special thanks to M. A. Michalick for CMOS circuit discussion and V. Thiantamrong for graphic editing.

## REFERENCES

- [1] A. Tuantranont, V. M. Bright, W. Zhang, and Y. C. Lee, "Flip chip integration of lenslet arrays on segmented deformable micromirrors," SPIE DTM'99 Vol.3680, pp.668-678, 1999.
- [2] J. Marshall, M. Gaitan, M. Zaghoul, D. Novotny, V. Tyree, J.I. Pi, C. Pina, and W. Hansford, "Realizing suspended structures on chips fabricated by CMOS foundry processes through the MOSIS service," NISTIR 5402, 1999.
- [3] B. C. Read, V. M. Bright, and J. H. Comtois, "Mechanical and optical characterization of thermal microactuators fabricated in a CMOS process," SPIE Vol. 2642, pp.22-32, 1995.
- [4] W. H. Chu, M. Mehregany, and R.L. Mullen, "Analysis of tip deflection and force of a bimetallic cantilever microactuator," J. Micromech. Microeng. 3, pp.4-7, 1993.